Radiology Case Reports 14 (2019) 595–601

Available online at www.sciencedirect.com

ScienceDirect

journal homepage: www.elsevier.com/locate/radcr

Case Report

A case of pseudocystic liver metastases from an atypical lung carcinoid tumor

Kazuhiko Morikawa, MD[a,], Takao Igarashi, MD, PhD[a], Shigeki Misumi[a], Taiki Fukuda[a], Hiroya Ojiri, MD, PhD[a], Hideki Matsudaira, MD[b], Hiroaki Shiba, MD, PhD[b], Shun Sato, MD[c]*

[a] *Department of Radiology, The Jikei University School of Medicine, Tokyo, Japan*
[b] *Department of Surgery, The Jikei University School of Medicine, Tokyo, Japan*
[c] *Department of Pathology, The Jikei University School of Medicine, Tokyo, Japan*

ARTICLE INFO

Article history:
Received 19 January 2019
Revised 20 February 2019
Accepted 23 February 2019
Available online 6 March 2019

Keywords:
Lung carcinoid tumor
Neuroendocrine tumor
Carcinoid metastasis
Liver metastasis
Pseudocyst

ABSTRACT

Metastatic neuroendocrine tumors of the liver typically appear as solid, hypervascular masses on imaging. Pseudocysts mimicking simple cysts are extremely rare. A 42-year-old Japanese woman was referred with a single pulmonary mass in the left lower lobe. No metastatic lesion was detected and no occupying lesion in the liver was observed. The lung tumor was diagnosed as an atypical carcinoid. Postoperative investigation revealed new hepatic simple cysts in the liver, which increased in size over time and changed into hemorrhagic cysts. Fluorodeoxyglucose positron emission tomography and somatostatin receptor scintigraphy using ^{111}In-octreotide demonstrated no accumulation in the liver. Our patient did not have symptoms consistent with carcinoid syndrome. The patient underwent partial resection of the cystic lesions of the liver. Gross examination of the tumors demonstrated thin-wall cavitated lesions with hemorrhage which were metastases from the atypical carcinoid of the lung. When a growing cystic lesion with intracystic hemorrhage is found in the liver of a patient with a history of carcinoid tumors, pseudocysts caused by degeneration of a carcinoid metastasis should be considered as a differential diagnosis.

Introduction

Neuroendocrine tumors (NETs) comprise a heterogeneous group of malignancies that arise from neuroendocrine cells throughout the body and most commonly originate from the lung, small intestine, and rectum. Lung NETs originate from pulmonary neuroendocrine cells that occur as individual cells or small pulmonary neuroendocrine cell clusters (neuroepithelial bodies) [1]. Lung NETs can be classified into 4 subtypes: well-differentiated, low-grade typical carcinoids; well-differentiated, intermediate-grade atypical carcinoids; poorly differentiated, high-grade large cell neuroendocrine carcinomas; and poorly differentiated, high-grade small cell lung carcinomas [1,2]. Although carcinoid tumors are considered low- or intermediate-grade tumors, they metastasize to regional lymph nodes and distant organs, and the most common sites of metastases are the liver and bone [1,3,4].

* Corresponding author.
E-mail address: k.morikawa@jikei.ac.jp (K. Morikawa).
https://doi.org/10.1016/j.radcr.2019.02.022

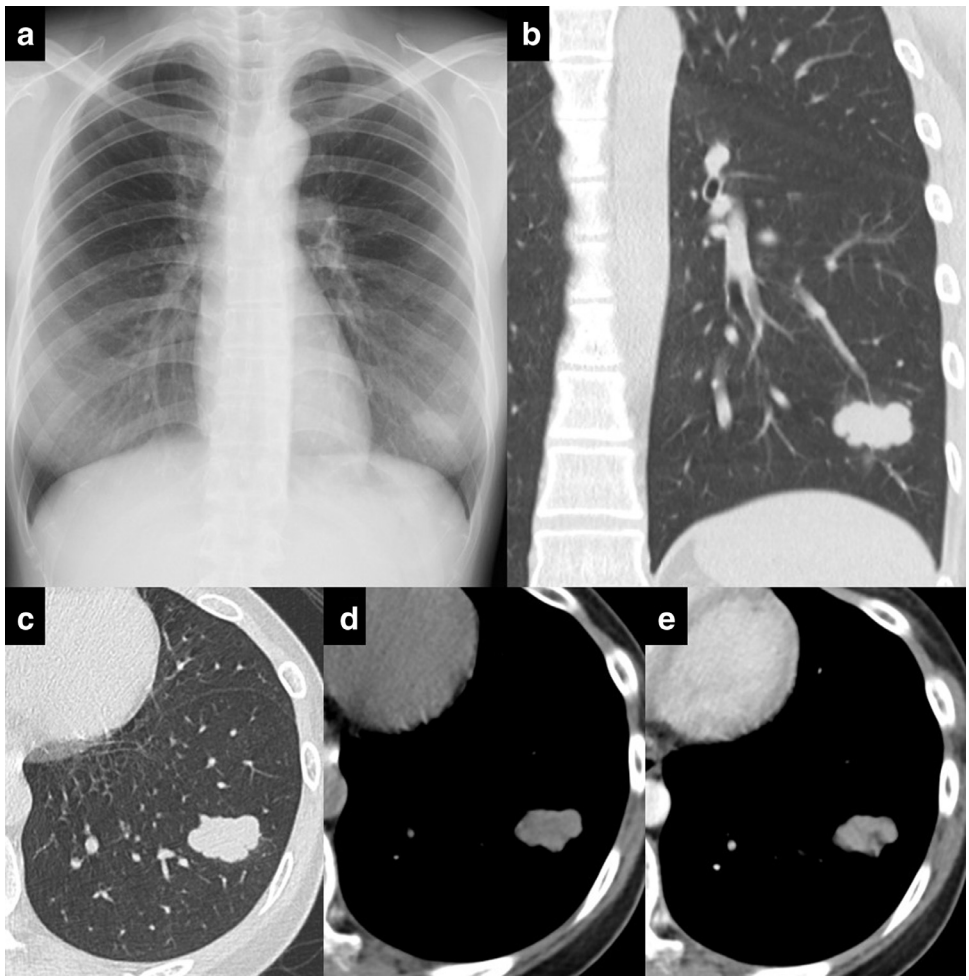

Fig. 1 – Chest radiograph and contrast-enhanced computed tomography (CT) of the chest obtained at the initial presentation. (a) Chest radiograph shows a solid lobulated tumor in the left lower lung field. Coronal (b) and axial (c) CT images show a 3 cm, lobulated solid tumor in the left lower lobe. Pre- (d) and post- (e) contrast-enhanced CT images show homogenous enhancement of the tumor.

The typical radiological presentation of lung carcinoid tumors and NETs in the gastrointestinal tract and liver (including metastases) is well known in the literature. The imaging findings of metastatic NETs in the liver are typically solid and hypervascular; those presenting with a cystic component are uncommon [4–6]. Furthermore, those with pseudocystic morphology mimicking simple cysts are extremely rare. We present a case of pseudocystic liver metastases mimicking simple cysts after resection of an atypical lung carcinoid tumor.

Case report

A 42-year-old Japanese woman was referred with a single pulmonary mass, which was discovered during a medical checkup. She had no symptoms of fever, cough, dyspnea, chest pain, hemoptysis, or diarrhea. She had no past medical history. She was an ex-smoker of 10 cigarettes per day for 10 years. Routine laboratory investigations were within normal limits and levels of serum tumor markers, including SCC, CEA, CA19-9, NSE, and AFP, were normal. Chest computed tomography (CT) revealed a solid lobulated tumor 3 cm in diameter in the left lower lobe and contrast-enhanced CT showed homogenous enhancement within the tumor (Fig. 1). No metastatic lesion was detected on whole-body survey and there was no occupying lesion in the liver. Left lower lobectomy under video-assisted thoracic surgery with regional lymph node resection was performed. Histopathological examination of the surgical specimen showed several growth patterns including nesting, cord-like pattern, rosette formation, and peripheral palisading of tumor nests (Fig. 2a). The tumor was composed of polygonal and spindle cells with round and oval-shaped nuclei, granular nuclear chromatin, and eosinophilic cytoplasm (Fig. 2b). Necrosis was absent. Immunohistological staining was positive for synaptophysin, chromogranin A, and CD56 (Fig. 2c-e). Mitotic figures were counted as 4 mitoses per 2 mm^2 (Fig. 2b). Based on these findings, the tumor was diagnosed as an atypical

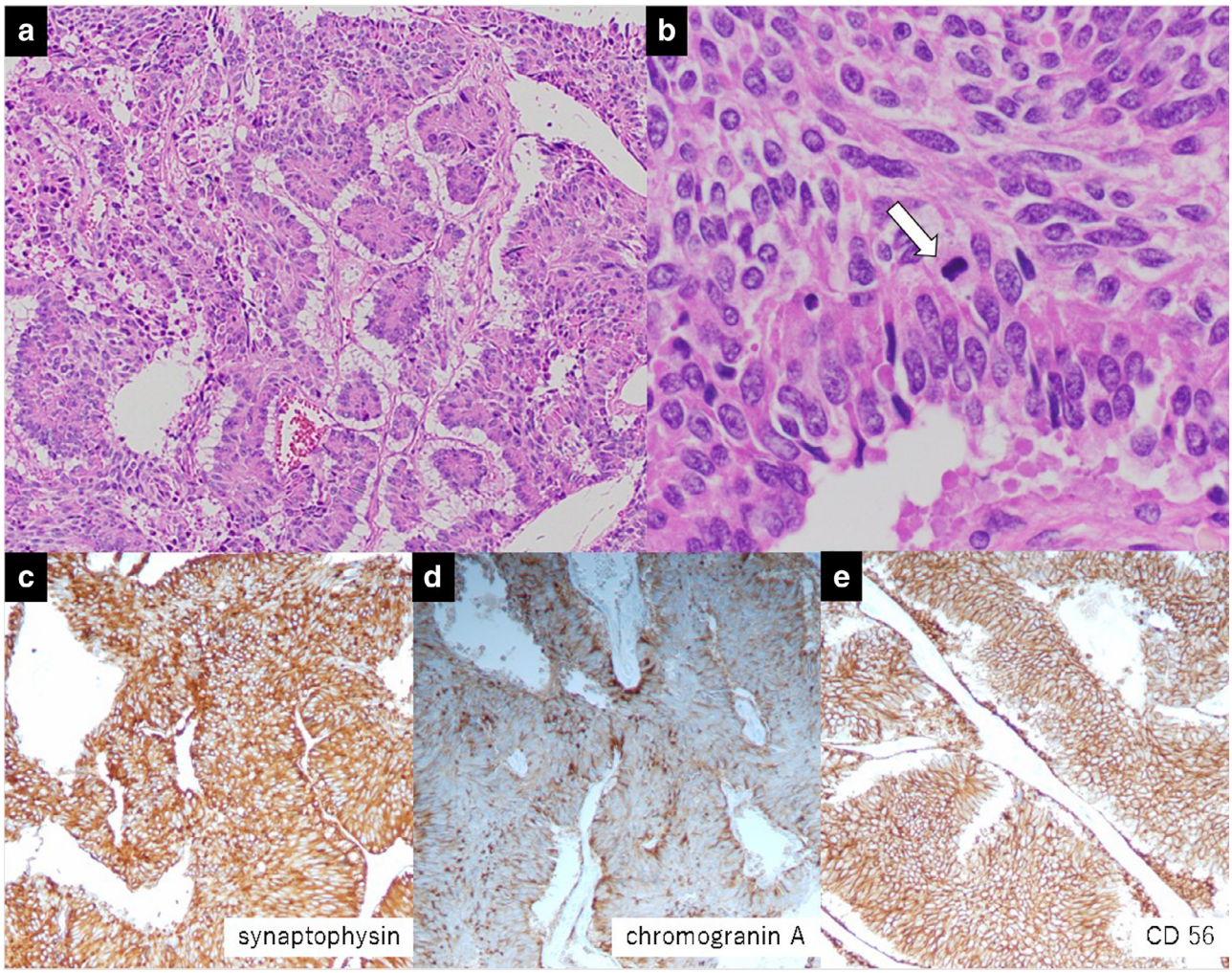

Fig. 2 – Histopathological examination of the lung tumor. (a) **Photomicrograph (original magnification, 100×; hematoxylin and eosin staining) shows characteristic neuroendocrine morphology including nesting, cord-like pattern, rosette formation, and peripheral palisading of tumor nests.** (b) **The tumor is composed of polygonal and spindle cells with round and oval shaped nuclei, granular nuclear chromatin, and eosinophilic cytoplasm. Mitosis is also observed at higher magnification (original magnification 400×; arrow). Immunohistological staining (original magnification, 100×) is positive for synaptophysin** (c)**, chromogranin A** (d)**, and CD56** (e)**.**

carcinoid. Intraoperative and histopathological staging was pT1cN0.

A year after the initial presentation, a routine screening with chest and abdominal CT revealed small cysts in hepatic segments 2 and 8 which were not detected on preoperative imaging (Fig. 3a and b). Another 6 months later (1.5 years after the initial presentation), the hepatic cysts increased in size (Fig. 3c and d). Ultrasound revealed well-margined simple cysts with thin walls and no solid component (Fig. 4). A year and 9 months after the initial presentation, magnetic resonance imaging of the liver revealed cysts with thin walls in segments 2 and 8 (Fig. 5). The cysts showed a homogeneous signal of slightly low intensity on T1-weighted images and markedly high signal intensity with a small amount of fluid-fluid level on T2-weighted images, suggesting intracystic hemorrhage. These hepatic lesions were identified as simple cysts when the lesions were first detected through imaging examination after lung lobectomy, but they increased in size over time and changed to hemorrhagic cysts. Two and a half years after the initial presentation (2.5 years after the lung lobectomy), the hemorrhagic cysts increased in size; however, a contrast-enhanced dynamic study showed no solid component within the cysts (Fig. 6b and c). Positron emission tomography performed with fluorine 18 fluorodeoxyglucose (FDG) did not reveal hypermetabolic activity of the lesions (Fig. 6d). Somatostatin receptor scintigraphy using ^{111}In-octreotide demonstrated no accumulation in the liver (Fig. 6e and f). Plasma chromogranin and urinary 5 hydroxyindoleacetic acid were not tested because our patient did not have symptoms consistent with carcinoid syndrome. Considering the higher recurrence rate of atypical carcinoids than that of typical carcinoids, the patient underwent a partial resection of the cystic lesion in hepatic segment 2 for diagnosis. Gross examination of the tumor showed a 13 mm cavitated

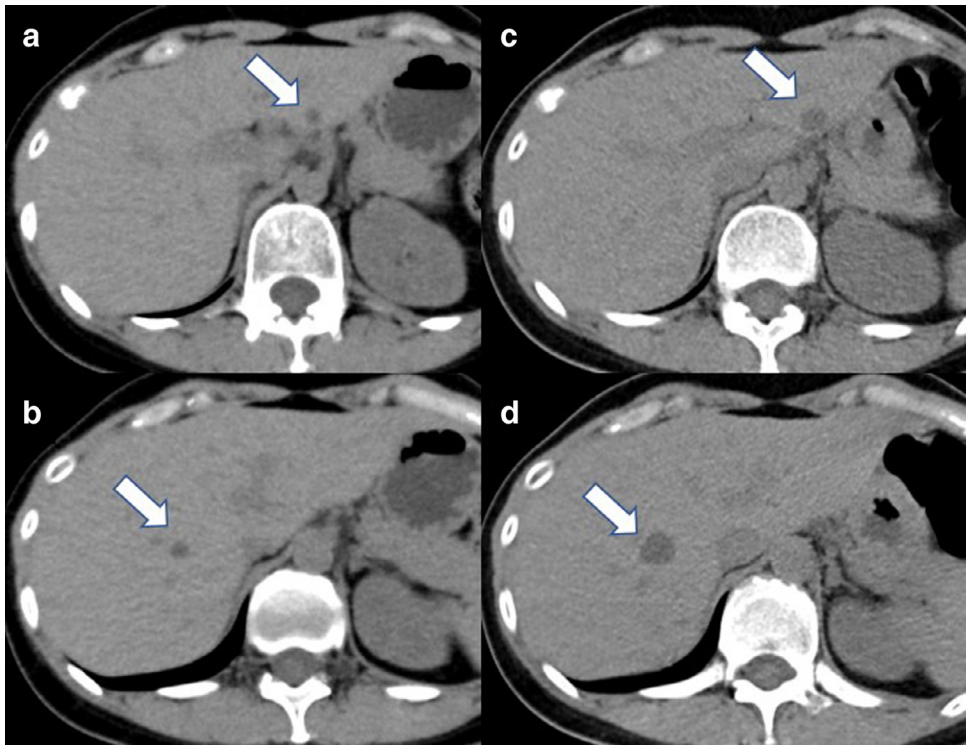

Fig. 3 – Computed tomography (CT) of the liver obtained 1 and 1.5 years after the initial presentation
CT shows small cysts (arrows) in segments 2 (a) and 8 (b) of the liver 1 year after the initial presentation. Six months later, the hepatic cysts (arrows) in segments 2 (c) and 8 (d) of the liver increased in size.

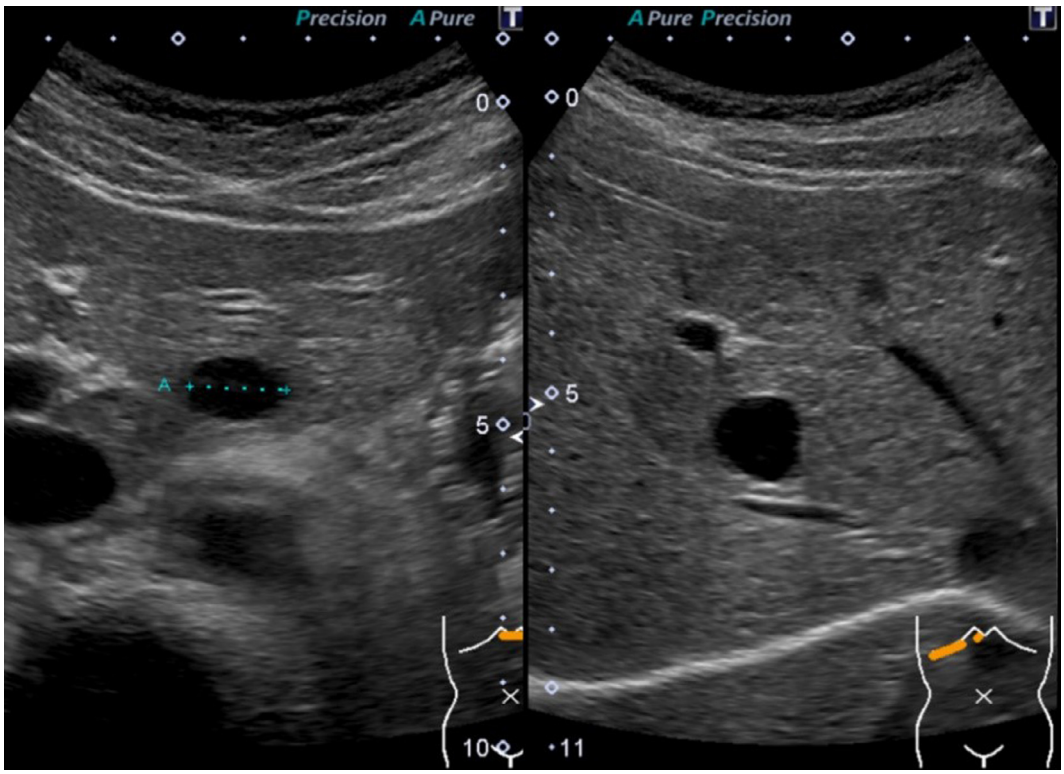

Fig. 4 – Ultrasound (US) of the liver obtained at the same time as the computed tomography in Figure 3
US shows a well-margined simple cyst with a thin wall with no solid component.

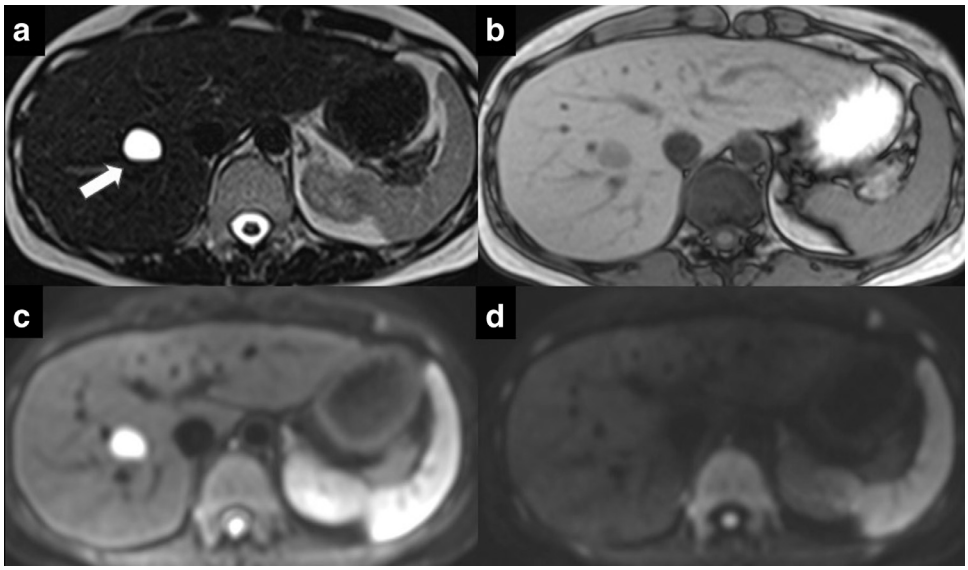

Fig. 5 – Magnetic resonance imaging of the liver obtained after ultrasound (1 year and 9 months after the initial presentation). (a) **T2-weighted image shows markedly high signal intensity with a small amount of fluid-fluid level in the cyst (arrow), suggesting intracystic hemorrhage.** (b) **T1-weighted image shows the cyst as homogenous, with slightly low signal intensity. Diffusion-weighted images show the cyst as having markedly high signal intensity on low b value (c), and low signal intensity on high b value (b = 1000)** (d).

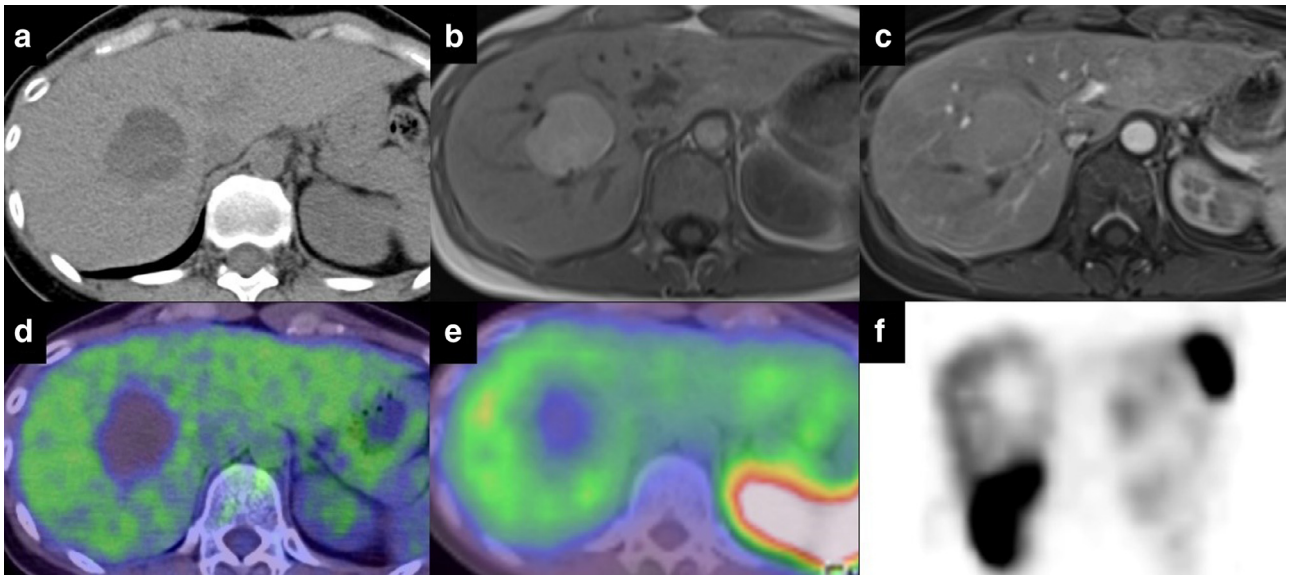

Fig. 6 – Images of the liver obtained 2.5 years after the initial presentation. (a) **Computed tomography (CT) shows a homogenous high attenuation mass in segment 8 of the liver.** (b) **T1-weighted image shows homogenous high signal intensity.** (c) **Gadolinium-enhanced fat-suppressed T1-weighted image shows no enhancement, suggestive of hemorrhage.** (d) **Axial fluorodeoxyglucose positron emission tomography (FDG-PET)/CT shows hypometabolic activity of the lesion. Axial single-photon emission computed tomography (SPECT)/CT image obtained with ^{111}In-octreotide** (e) **and planer image** (f) **show defects in accumulation consistent with the cystic lesion of the liver.**

lesion with hemorrhage. Histopathologically, the tumor cells inside the tumor fell into a wide range and the tumor cells presented the same appearance as those from the lung tumor, with positive immunohistological staining for synaptophysin, chromogranin A, and CD56. These findings indicated that the hepatic lesion was a metastasis from the atypical carcinoid of the lung. A month after the partial resection of hepatic segment 2 for diagnosis, right lobectomy was performed. Gross examination of the tumor demonstrated a 45 mm remarkably cavitated lesion with hemorrhage with no solid component. It

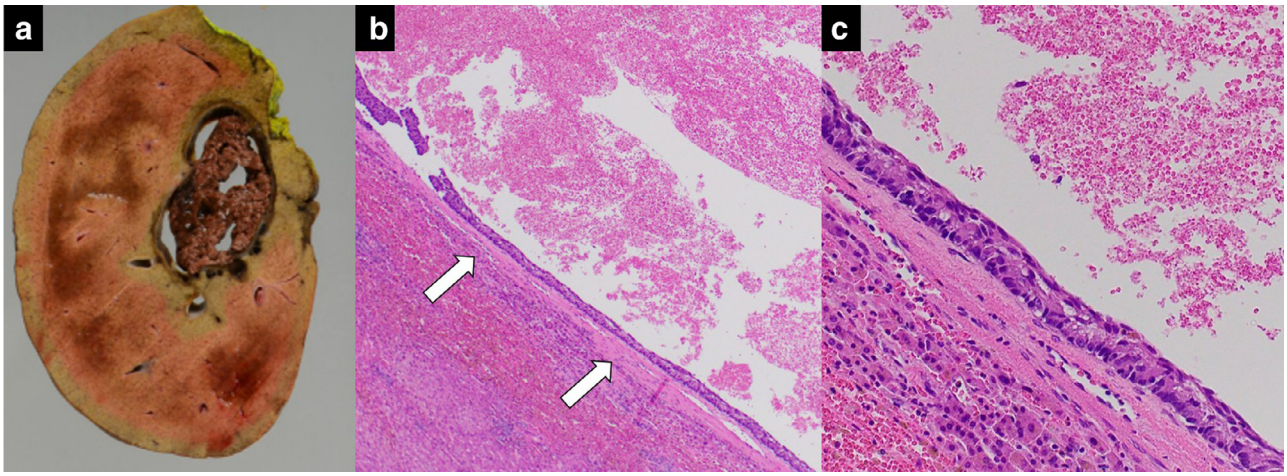

Fig. 7 – Sectioned gross specimen and histopathological findings of surgical specimen of the liver. (a) Gross examination of the tumor demonstrates a remarkably cavitated lesion with hemorrhage. (b) Hematoxylin and eosin staining. Lower magnification (40×) of the sectioned specimen shows a blood-filled cyst with a thin wall consisting of a few layers of the tumor cells (arrows). (c) Higher magnification (100×) of the same tumor shows nesting and cord-like growth pattern similar to that of the lung specimens.

was also proven to be a metastatic liver tumor histopathologically (Fig. 7). There was no local recurrence of either the lung or liver tumor during the half year following surgery.

Discussion

Carcinoid tumors are characterized by bland polygonal or spindled cells with scant cytoplasm and finely granular chromatin arranged in organoid nests, trabeculae, or cords. Typical carcinoids are defined as lung carcinoid tumors measuring at least 0.5 cm with fewer than 2 mitoses per 2 mm^2 of viable area of tumor and lacking necrosis, whereas atypical carcinoids have 2-10 mitoses per 2 mm^2 of viable area of tumor, often with the presence of focal necrosis [1–5,7]. The updated 2015 World Health Organization classification for lung NETs also provides guidance on use of the Ki-67 cell proliferation labeling index to distinguish between high-grade lung NETs (>40%) and carcinoids (<20%) [1,2]. The expressions of neuron-specific enolase, chromogranin, and synaptophysin as neuroendocrine markers are valuable in terms of identifying neuroendocrine features and are the most useful markers for differentiating NETs from nonendocrine poorly differentiated adenocarcinoma [1–7].

The imaging features of typical and atypical lung carcinoids are similar. Central carcinoids are often near the tracheal bifurcation and are seen as small nodules entirely located within the lumen of a bronchus. Sometimes, they can cause distal obstructive atelectasis, pneumonitis, or mucus plugging. Peripheral carcinoids usually measure less than 3 cm, may not show a bronchial relationship, and appear as well-defined lobulated nodules or masses, sometimes with necrosis when the tumor is large. Both typical and atypical carcinoids show good contrast enhancement on CT (>30 HU) and may be associated with reactive or metastatic hilar or mediastinal lymphadenopathy [3,4].

Metastases occur in 15% of typical carcinoid tumors and 30%-50% of atypical carcinoid tumors of the lung, and usually involve the liver, bone, adrenal glands, and brain [4]. The liver is the most common site of NET metastasis and gastrointestinal NETs are the most common primary tumors of these metastases (37%-55% of cases) [4]. However, in a minority (5%-14%) of patients with NET liver metastases, the primary tumor cannot be identified [7].

Metastatic NETs of the liver typically appear as solid, hypervascular masses on imaging. The typical imaging presentation of NETs in the liver (including metastases) are solid and hypervascular. With contrast-enhanced imaging, tumors show marked contrast-enhancement in the arterial and portal phases and commonly show a major lesion surrounded by several satellite nodules [4]. The arterial hyperenhancement is due to a rich hepatic arterial supply [4]. On magnetic resonance imaging, NETs in the liver have low signal intensity on T1-weighted images and high signal intensity on T2-weighted images [5].

Earlier reports have described that NETs in the liver are typically solid and can be accompanied by cystic components [6]. However, metastatic NETs of the liver rarely present as pseudocystic or predominantly cystic masses. The imaging findings of a pseudocystic lesion of the liver, in the absence of clinical symptoms, can imply several differential diagnoses, ranging from infectious diseases such as echinococcal cysts and benign lesions such as simple biliary cysts and biliary cystadenomas, to primary or metastatic malignancies [7]. Cystic hepatic metastases may occur due to necrosis and cystic degeneration of rapidly growing hypervascular tumors or as a manifestation of mucinous colonic or ovarian adenocarcinomas [8]. Our search of the English literature yielded 12 case reports that described pseudocystic or predominantly cystic liver metastases [6,7,9–15], and we evaluated the clinical features and imaging findings of these cases. This group consisted of 4 men and 8 women with a mean age of 60 years (range, 48-68). Of the patients who were symptomatic (11/12

cases, 92%), 42% (5/12 cases) presented with typical carcinoid syndrome, such as flushing and diarrhea, 33% (4/12 cases) presented discomfort of the abdomen and/or a palpable hepatic mass, and 25% (3/12 cases) presented abdominal pain and discomfort of the abdomen. A single nodule (with or without several small satellites) ranged in size from 7 cm to 20 cm in diameter (a measurement of the size of the nodule was given in only 10 cases). Tumors were detected as a pseudocystic mass in 9/12 cases; however, tumors detected as a cystic mass contained a solid component in the published images in 3/12 cases. These previous reports concluded that the pseudocystic appearance of the metastasis tumor was due to central necrosis or intratumoral hemorrhage from macroscopic and microscopic examination, as with our case. The increase in size of hepatic cysts which appeared after the resection of carcinoid tumors increase and the detection of intracystic hemorrhage were findings suspect of pseudocystic metastases.

The primary lesion was detected in 5 cases (42%) and they all originated from the ileum. To the best of our knowledge, this is the first report of pseudocystic metastases of the liver from an atypical lung carcinoid tumor that were found as simple cysts at first and which changed to hemorrhagic cysts over time.

With FDG-positron emission tomography, NETs both exhibit lower FDG uptake than expected for malignant tumors and show increased FDG uptake associated with their high metabolic activity and malignant potential [3]. In our patient, we did not detect increased FDG uptake by the liver tumors. The absence of increase in FDG uptake was seemingly caused by remarkable cystic degeneration with hemorrhage and a scarce solid component.

Somatostatin receptor scintigraphy using ^{111}In-octreotide is the most widely used technique for the evaluation of NETs as it can reveal radiologically occult lesions and unsuspected metastatic disease [3,4]. A previous case report has shown a liver mass mainly with a cystic component which revealed no accumulation with somatostatin receptor scintigraphy [7].

Surgical resection is the only curative treatment for resectable lung carcinoid tumors. The preferred treatments are lobectomy and pneumonectomy. Surgery may also be considered in patients with advanced/metastatic disease, and complete surgical resection of the primary tumor and metastases can often be recommended [1]. Complete resection of NET liver metastases leads to an improved prognostic outcome: 5-year overall survival rates higher than 70% are reported, despite recurrences developing in up to 80% of patients. Thus, the rationale to remove NET liver metastases, once technically feasible, is established [5].

Conclusion

Cystic degeneration of metastatic liver carcinoid tumors may occur due to ischemic necrosis or intratumoral hemorrhage of the tumor. When a growing cystic lesion is found in the liver of a patient with a history of lung carcinoid tumors, pseudocysts caused by cystic degeneration of a carcinoid metastasis should be considered as a differential diagnosis.

Conflicts of interest

We wish to confirm that there are no known conflicts of interest associated with this publication and there has been no significant financial support for this work that could have influenced its outcome.

REFERENCES

[1] Hendifar AE, Marchevsky AM, Tuli R. Neuroendocrine tumors of the lung: current challenges and advances in the diagnosis and management of well-differentiated disease. J Thorac Oncol 2016;12(3):425–36. doi:10.1016/j.jtho.2016.11.2222.

[2] Travis WD, Brambilla E, Burke AP, Marx A, Nicolson AG. WHO classification of tumours of the lung, pleura, thymus and heart. 4th ed. Lyon, France: International Agency for Research on Cancer; 2015.

[3] Chong S, Lee KS, Chung MJ, Han J, Kwon OJ, Kim TS. Neuroendocrine tumors of the lung: clinical, pathologic, and imaging findings. Radiographics 2006;26(1):41–58. doi:10.1148/rg.261055057.

[4] Baxi AJ, Chintapalli K, Katkar A, Restrepo CS, Betancourt SL, Sunnapwar A. Multimodality imaging findings in carcinoid tumors: a head-to-toe spectrum. Radiographics 2017;37(2):516–36. doi:10.1148/rg.2017160113.

[5] Scarsbrook AF, Ganeshan A, Statham J, Thakker RV, Weaver A, Talbot D, et al. Anatomic and functional imaging of metastatic carcinoid tumors. Radiographics 2007;27(2):455–77. doi:10.1148/rg.272065058.

[6] Salamone L, McCarthy S, Salem RR. Atypical cystic carcinoid tumors of the liver. J Clin Gastroenterol 2010;44(10):e256–9. doi:10.1097/MCG.0b013e3181da7714.

[7] Fiori S, Del Gobbo A, Gaudioso G, Caccamo L, Massironi S, Cavalcoli F, et al. Hepatic pseudocystic metastasis of well-differentiated ileal neuroendocrine tumor: a case report with review of the literature. Diagn Pathol 2013;8:148. doi:10.1186/1746-1596-8-148.

[8] Vachha B, Sun MRM, Siewert B, Eisenberg RL. Cystic lesions of the liver. Am J Roentgenol 2011;196:W355–66. doi:10.2214/AJR.10.5292.

[9] McDermott EWM. Metastatic carcinoid tumour presenting as a hepatic pseudocyst. Ir J Med Sci 1987;156(5):149–50. doi:10.1007/BF02953233.

[10] Silvain C, Besson I, Azaïs O, le Bezu MW, Morichau-Beauchant M. Pseudocystic hepatic metastasis: unusual onset of carcinoid tumor. Dig Dis Sci 1991;36(4):542–3.

[11] Prvulovich EM, Stein RC, Bomanji JB, Ledermann JA, Taylor I, Ell PJ. Iodine-131-MIBG therapy of a patient with carcinoid liver metastases. J Nucl Med 1998;39(10):1743–5.

[12] Lemaire LC, Pols HA, Tilanus HW. Carcinoid tumour presenting as a giant hepatic cyst. Br J Surg 1995;82(1):133.

[13] Dent GA, Feldman JM. Pseudocystic liver metastases in patients with carcinoid tumors: report of three cases. Am J Clin Pathol 1984;82(3):275–9.

[14] Isomura T, Kojira M, Kawana J, Nakamura S, Naito H, Yoshida K, Nakayama Y, Nakayama T, Kubo Y. Small multiple carcinoid tumors occurring in the ileum with a pseudocystic liver metastasis. Acta Pathol Jpn 1980;30(1):137–43.

[15] Wijesuriya SR, Siriwardana R, Deen K. Education and Imaging. Hepatobiliary and pancreatic: carcinoid tumor with cystic liver metastases. J Gastroenterol Hepatol 2010;25(3):647. doi:10.1111/j.1440-1746.2010.06290.x.